INVESTIGATION OF THE MORPHOLOGY AND OPTICAL PROPERTIES OF $CuAlO_2$ THIN FILM

BY

AMINU TUKUR MOHAMMED

SPS/12/MPY/00007

BSc Ed, PGDIP

A DISSERTATION SUBMITTED TO THE DEPARTMENT OF PHYSICS BAYERO UNIVERSITY KANO, IN PARTIAL FULFILMENT OF THE REQUIREMENTS FOR THE AWARD OF A DEGREE OF MASTER OF SCIENCE (M.Sc.) IN ELECTRONICS.

MARCH, 2016

DECLARATION

I hereby declare that this work is the product of my research efforts undertaken under the supervision of Dr Tijjani H. Darma and Dr Abdu Yunusa and has not been presented anywhere for the award of degree or certificate. All sources have been duly acknowledged.

Signature and Date

Aminu Tukur Mohammad

(SPS/12/MPY/00007)

CERTIFICATION

This is to certify that the research work for this dissertation and the subsequent write-up by Aminu Tukur Mohammad with registration number SPS/12/MPY/00007, were carried out under my supervision.

Signature……..

Dr T. H. Darma

Signature…….

Dr Abdu Yunusa

Signature…….

Dr T. H. Darma
H.O.D physics

APPROVAL PAGE

This dissertation has been examined and approved for the award of Master of Science in Electronics. (Msc. Electronics)

Sign…… ……

Prof. Nasiru Rabiu Date
(External Examiner)

Sign…… ……

Dr Abdu Yunusa Date
(Internal Examiner)

Sign…… ……..

Dr. T. H. Darma Date
(Supervisor)

Sign…… …….

Dr. T. H. Darma
(H.O. D Physics) Date

ACKNOWLEDGEMENT

All praise is to Allah the most beneficent the most merciful who in His infinite mercy makes this work a reality. Praise and salutations also goes to our Prophet, Muhammad (S.A.W.) his family and Sahaba and all those that follow his righteous path.

I am highly indebted to my Father Alhaji Mohammad Amama (May his gentle soul rest in perfect peace) who set me on the path to struggle and not give up in life no matter how hard the situation appears to be, his advice and guidance has been of great help to me such that no words can adequately describe my feeling of indebtedness to him. A special gratitude goes to my supervisor Dr. T. H. Darma and my Internal Supervisor Dr. Abdu Yunusa were constantly helping and encouraging me throughout this work. My appreciation also goes to the P.G Coordinator Prof. B. I. Tijjani and the former post graduate coordinator Dr. Muktar Aliyu and the entire staff of Physics Department Bayero University, Kano.

My special appreciation also goes to my two wives Asmau and Hajara as well as my children for their patience and endurance during this work. I am also obliged to my course mates and working mates in the Jigawa state polytechnic, Dutse especially Abdu Barde, Salisu Ahmed, and Salisu Isyaku who have been of help in one way or the other towards the success of this work.

DEDICATION

This research work is dedicated to my late Father and Mother Alhaji Mohammad Amama and M. Sa'adatu Adamu may their gentle souls rest in peace (Amin)

TABLE OF CONTENTS

Declaration i
Certification ii
Approval Page iii
Acknowledgement iv
Dedication v
Abstract ix
CHAPTER ONE 1
1.0 Introduction 1
1.1 Transparent Conducting Oxides (TCOS) 2
1.2 Statement of The Problem 2
1.3 Aim and Objectives 2
1.3.1 Aim 2
1.3.2 Objective 3
CHAPTER TWO 4
2.0 Literature Review 4
2.1 Classification of TCO Materials 4
2.1.1 P-Type TCO 5
2.1.2 $CuAlO_2$ as P-type TCO 6
2.2 Thin Film Deposition Techniques 8
2.2.1 Chemical Deposition 8
2.2.2 Plating 9
2.2.3 Spin Coating 9
2.2.4 Chemical Vapor Deposition (CVD) 9
2.2.5 Plasma Enhanced (PED) 9
2.2.6 Atomic Layer Deposition (ALD) 10
2.2.7 Chemical Solution Deposition 10
2.3 Optical Properties of Thin Film 10
2.4 Absorbance 12
2.5 The Absorption Coefficient 13
2.6 Fourier Transform Infrared (FT-IR) Spectroscopy 14
CHAPTER THREE 16

3.0 Materials and Method 16
3.1 Materials 16
3.2 Method 16
3.2.1 Sol-Preparation 16
3.2.2 Substrate Preparation 17
3.3 Coating Process 17
3.4 Annealing Process 18
3.5 Study of The Surface Morphology 18
3.5.1 The SEM Measurements 18
3.5.2 SEM Components and Operation 19
3.5.3 Magnification and Image Formation 20
3.5.4 Samples Preparation for SEM Measurements 21
3.6 Study of The Optical Characteristics 21
3.7 UV-Visible Spectrophotometer 22
3.7.1 The Working Principle Of UV-VIS Spectrophotometer 22
3.7.2 Sample Preparation for UV-Measurements 23
3.8 Fourier Transform Infrared (FT-IR) Spectroscopy 24
3.8.1 Components Principles and Measurement of FT-IR Spectrometer 24
3.8.2 Sample Preparation for FT-IR Spectrometer Measurement 25
CHAPTER FOUR 26
4.0 Result and Discussion 26
4.1 Study of The Optical Properties 28
4.1.3 Absorption Coefficient 34
4.1.4 Energy Band Gap 35
4.1.5 Direct Band Gap 36
4.1.6 The Extinction Coefficient 37
4.2 Fourier Transform Analysis of The $CUALO_2$ Thin Film 38
4.2.1 Absorbance in FT-IR Spectroscopy 38
4.2.2 Transmittance in FT-IR Spectroscopy 39
CHAPTER FIVE 41
5.0 Summary, Conclusion and Recommendation 41

5.1 Summary 41
5.2 Conclusion..... 43
5.3 Recommendations for Further Research 44
Reference:..... 45

ABSTRACT

In this work p-type TCO was developed using the chemical solution deposition (sol-gel) method, with CuCl and $AlCl_3$ taken as the starting materials. The prepared sol was deposited on glass substrate. Five samples were produced out of which four were annealed at different temperatures for 2 hours. The SEM measurements of the annealed samples revealed an improved crystallinity with increasing annealing temperature. The results of the UV-Vis and FT-IR spectrophotometry indicate that while transmittance and direct band gaps vary directly with annealing temperature, the absorbance decreased sharply from a common value of about 89% at about 329nm to a range of values of 56.2%-35.2%. The absorption coefficient decreased with increase in annealing temperature from 1.58 x 10^{-6} cm^{-1}, 1.29 x 10^{-6} cm^{-1} and 1.08 x 10^{-6} cm^{-1} at about 1.14eV in the infrared region to about 1.93 x 10^{-6} cm^{-1}, 1.58 x 10^{-6} cm^{-1}, and 1.29 x10^{-6} cm^{-1} at about 3.62e in the visible region, the extinction coefficient for all the samples decreased from 133.89 x $10^{-3}cm^{-1}$ 111.76^{-3} x 10 $^{-3}cm^{-1}$,93.45 x$10^{-3}cm^{-1}$ and 89.44 x $10^{-3}cm^{-1}$ in the infrared region to about 81.11 x $10^{-3}cm^{-1}$, 82.22 x$10^{-3}cm^{-1}$, 83.35 x $10^{-3}cm^{-1}$ and 84.42 x$10^{-3}cm^{-1}$ at about 4.05eV in the visible region. The deposited films were found to be suitable for optoelectronics applications.

CHAPTER ONE

1.0 INTRODUCTION

Transparent conducting oxides (TCO) thin films of In_2O_3, ZnO, SnO_2 , $CuAlO_2$ etc. and their mixtures have been extensively used in optoelectronic applications such as transparent electrodes in touch panels, flat panel displays (FPDs), infrared detectors solar cells, gas detectors and many other applications. This chapter provides an introduction to the basic physics of TCO films and surveys the various topics and challenges in the field and the technology behind the fabrications. TCOs are very useful materials to transparent optoelectronics because they have unique features of optical properties in the visible light region such as the transparency over 85% and optical band gap greater than 3eV and controllable electrical conductivity such as carrier concentration of at least $10^{20}cm^{-3}$ and resistivity of about $10^{-4}\Omega cm$ (Kim, *et al.,* 2011).Since the discovery of p-type conductivity in $CuAlO_2$ many Cu (I) based delafossites having transparency and p-type conductivity have been synthesized. After the report of p-type semiconducting transparent $CuAlO_2$thin film, a new field in device technology called the 'transparent electronics' in which a combination of the two types of TCOs in the form of a p-n junction has emerged (Thomas,1997). This lead to a 'functional' window which would transmit visible potion of solar radiation yet generates electricity by the absorption of part UV. Also $CuAlO_2$ has good thermoelectric field-emission, ozone sensing, photochemical and photo-catalytic hydrogen evolution properties as well as ferromagnetic characteristics and capability of refrigeration of electronic devices (Roy ,*et al.,*2003). Also keeping an eye in the tremendous progress in Nanotechnology; fabrication and characterization of Nano-structure p-$CuAlO_2$ as well as other p-TCO thin films have become an important field of work, because of new and interesting properties exhibited by these Nano materials (Banerjee and Chattopadhyay, 2005).

1.1 TRANSPARENT CONDUCTING OXIDES (TCOS)

Transparent conductive oxides (TCOs) are doped metal oxides used in photovoltaic devices such as flat panel displays and photovoltaics (including inorganic devices, organic devices, and dye-sensitized solar cell). Most of these films are fabricated with polycrystalline or amorphous microstructures (Minami, 2005). Typically these applications use electrode materials that have greater than 80% transmittance of incident light as well as electrical conductivities higher than 10^3S/cm for efficient carrier transport. (Minami, 2005)

1.2 STATEMENT OF THE PROBLEM

Several researches were conducted on the fabrication and characterization of $CuAlO_2$ thin films using different deposition techniques such as pulse laser deposition, wet dip chemical coating, e beam method, magnetron sputtering and many others out of which the effect of varying annealing temperature on the morphology and optical properties of the deposited film through the use of UV-Vis and FT-IR need to be fully analyzed, this problem necessitates the effort to conduct the research and find out the extent to which the variation of annealing temperature affects the surface morphology and optical properties of $CuAlO_2$ thin film deposited using the chemical solution deposition (sol gel) process.

1.3 AIM AND OBJECTIVES

1.3.1 AIM

To prepare and investigate the morphology and optical properties of $CuAlO_2$ thin film

1.3.2 OBJECTIVES

The objective of this research work is

- To point out the depth or extent to which the sol gel or chemical solution method of thin film deposition is effective in the fabrication of $CuAlO_2$ thin film.
- To analyse and find out the annealing temperature that will be more suitable in producing smooth surface morphology with well-defined grain boundaries and good optical characteristics of $CuAlO_2$ thin film.
- To measure some of the optical properties such as absorbance, transmittance, absorption coefficients extinction coefficients and band gaps of the samples of $CuAlO_2$ thin film annealed at different temperatures.

CHAPTER TWO

2.0 LITERATURE REVIEW

The semiconducting delafossites-type oxides in the chemical form of $M^{I}M^{III}O_2$ where, $M^{I}$is a monovalent cation (e.g. Cu^{1},Ag^{1}) and M^{III} is a trivalent cation (e.g. Al^{III}, In^{III}, Cr^{III}, Co^{III}, Fe^{III} etc) have attracted renewed interest in the field of transparent conducting thin film technology after the report of p-type conductivity in the transparent thin film of $CuAlO_2$ (Kawazoe,*et al.,* 1997) Most of the well-known and commonly used transparent conducting oxides such as ZnO_{I-x}, In_{I-x} , Sn_xO_3 , SnO_2 : F/Sb/Mo , Cd_2SnO_4 etc. are n-type materials which are widely used in flat panel displays, solar cells and in many such applications (Cachet, 2001) . Transparent conducting oxides are widely applied as transparent electrodes in flat panel displays, solar cells and touch panels. The main hindrance for the versatile application of TCO devices is the absence of high conductivity p-type TCOs. However the delafossites structure $CuAlO_2$ film was first achieved in 1997 as a candidate to be a highly conductive p-type TCO (Kawazoe, *et al.,* 1997)

2.1 CLASSIFICATION OF TCO MATERIALS

Transparent conducting oxides are very useful materials to transparent optoelectronics because they have unique features of optical properties in the visible region such as the transparency over 85% and optical band greater than 3eV and controllable electrical conductivity such as carrier concentrations of at least $10^{20}cm^{-3}$ and resistivity of about 10^{-4} ohm cm (kim, *et al*.,2011) Notwithstanding their extraordinary wide controllable conductivity range including that of semiconductor behavior, their applications are in the transparent electrodes. It seems that the origin of these limited applications is due to a lack of p-type conducting transparent oxide materials. TCO materials are usually n-type semiconductors and the lack of a high quality p-type

TCO always has been the main obstacle in holding the fabrication of a fully transparent complementary metal oxide semiconductor-like devices.

Although n-type TCO such as ZnO, SnO_2 and ITO are key components in a variety of technologies, p-type TCO are emerging areas with little work previous to four years ago.(Coppo *et al.,*2004*)* However realization of good TCO could significantly impact a new generation of transparent electrical contacts for p-type semiconductors and organic optoelectronic materials in conjunction with n-type TCOs which could lead to a next generation of transparent electronics

2.1.1 P-TYPE TCO

Since the first report of p-type TCO on NiO, in 1997, there was a report of transparent p-type conducting films of $CuAlO_2$ showing considerable improvement over the NiO (Sato,*et al.,* 2003; Kawazoe, *et al.,* 1997) Although the conductivity of $1Scm^{-1}$ was about three orders of magnitude smaller than that of n-type materials the result was promising, following the discovery of p-type conductivity in $CuAlO_2$ many Cu(I) based delafossites having transparency and p-type conductivity have been synthesized, such as $CuScO_2$, $CuYO_2$, $CuInO_2$, $CuGaO_2$, and $CuCrO_2$ (Sunyoung, *et al.,2011*). Conductivity of the $CuInO_2$ film deposited under working Oxygen pressure of 7.5mTorr and 450ºC was reported as $2.8x10^{-3}$S/cm(Roy, et al., 2003) and also, the dependence of the electrical conductivity of $CuInO_2$ films upon the deposition temperature was investigated. With increasing deposition temperature from room temperature to 600ºC resulted in the conductivity increase which reaches a value of $5.8x10^{-2}$ S/cm for the film deposited at 400ºC temperature (Sunyoung, *et al.,* 2011). Indeed, other structures have been identified that combine p-type conductivity and optical transparency in Cu (I) based materials, including $SrCuO_2$ and oxychalogenides (LaCuOS), although to date the p-type TCO with the highest conductivity is a delafossites (Mg doped $CuCrO_2$), (Sunyoung, *et al.,2011*). Among various candidate materials,

ZnO is one of the most important members of TCOs. Like the other members (e.g.; SnO_2 ,In_2O_3, IZO and ITO) ZnO have been applied (Sunyoung, *et al.,* 2011).

2.1.2 $CuAlO_2$ AS P-TYPE TCO

Kawazoe, *et al*, (1997) first reported synthesis of $CuAlO_2$ as a p-type TCO material based on the copper I Oxides such as $CuAlO_2$, $CuGaO_2$,and $SrCuO_2$ with chemical modulation of valence band,in spite of several merits of $CuAlO_2$ as a P-type TCO , the main hurdle is its low electrical conductivity compared to the n-type TCO. Therefore, different methods such as high temperature solid state reaction, hydrothermal method ion exchanges and sol-gel methods etc. have been proposed to prepare $CuAlO_2$ (Ghosh, *et al*., 2009).Each copper atom in $CuAlO_2$ is linearly coordinated with two oxygen atoms toform an O-Cu-O dumbbell unit placed parallel to the c-axis. Oxygen atoms of the O-Cu-O dumbbell link Cu layers with the AlO_2 layers. For the synthesis of $CuAlO_2$ thin films, the groups of Hosono, Gong and Chattopadhyay used a pulsed laser deposition, plasma-enhanced metalorganic chemical vapor deposition and dc sputtering, respectively. (Sheng, *et al*., 2006) The electronic structures of $CuAlO_2$ were experimentally probed by normal/inverse photoemission spectroscopy. The Fermi energy determined experimentally was set to zero in the energy scale in the three spectra. A band gap was observed between the valance band edge in the photoemission spectroscopy and the conduction band edge in the Inverse photoemission spectroscopy, the band gap estimated was about 3.5eV. The Fermi energy lies around the top of the valance band. The origin of theFermi level was determined using Goldelectrode deposited on sample. These result means that $CuAlO_2$ is a transparent p-type semiconducting material, which has excellent potential for use in optoelectronics device technology.

Tanooka, and Kikuchi (2002) reported the synthesis of phase impure copper aluminium oxide films by solution method using metal alkaloids and nitrates as metal sources in the precursor solutions. Chen, *et al,.* (2000) used similar solution process to synthesize $CuAlO_2$ thin film using copper acetate and aluminium nitrate as metal sources. Guillen*et al.,*(2002) used organometallic compounds to fabricate both phase pure and phase impure copper aluminium oxideusing sol-gel process at different Cu/Al ratios.

Lam, *et al* (2009) conducted a research on the annealing effects on the structural, optical and electrical properties of $CuAlO_2$ thin film deposited by magnetron sputtering. He found that the crystallinity of $CuAlO_2$ is improved with increasing annealing temperature in N_2 ambient and the film annealed at 900^{o}C presents the excellent preferred (001) orientation in x-ray diffraction.

Kim, *et al.,* (2007) conducted another research on optical and electrical properties of p-type transparent conducting oxides $CuAlO_2$ thin film. In the work p-type transparent conducting $CuAlO_2$ thin film were prepared by e-beam evaporation and wet oxidation technique. In the work transmittance varied from 20- 85% and the resistivity from $5x10^{-3}$ to 4Ωcm with wet oxidation conditions. The nature of the p-type film was confirmed by the positive Hall Effect technique Optical band gap was estimated to be in the range 3.96-4.20eV.

Arghya, *et al.,* (2010) conducted a research on wet chemical dip coating preparation on highly oriented copper aluminium oxide thin film and its opto-electrical characterization. In the work transparent p-type semiconducting copper aluminium oxide thin film was synthesized by wet chemical route. The films were deposited by dip coating on Si and glass substrates. XRD pattern confirms the crystalline $CuAlO_2$ phase formation with strong (006) orientation while UV-Vis measurement shows a high transparency of the film in the region with direct band gap of 3.94ev.

Banerjee, *et al.,* (2005) conducted another research on the size dependent optical properties of sputter-deposited nanocrystalline p-type transparent $CuAlO_2$ thin film.He deposited nanocrystalline p-type semiconducting transparent $CuAlO_2$ thin films by direct current sputtering of a prefabricated polycrystalline $CuAlO_2$ target with deposition time as a variable parameter. Transmission electron micrographs reveal the formation of $CuAlO_2$ nanoparticles. X-ray diffraction shows some diffraction peaks depicting rhombohedral crystal structure. The band gap values obtained from the optical transmission and reflection data for the films deposited in 3and 9mins are 3.94 and 3.84eV respectively.

2.2 THIN FILM DEPOSITION TECHNIQUES

Most deposition techniques control layer thickness within few tens of nanometers. (Sheshan, 2012) Molecular beam epitaxy allows a single layer of atoms to be deposited at a time. It is useful in the manufacture of materials in such fields as optics (for reflective, anti-reflective coatings or self-cleaning glass, for instance) electronics (layers of insulators semi-conductors and conductors from integrated circuits) packaging (i.e. Aluminium-coated PET film), and in contemporary art. Similar processes are sometimes used where the thickness is not important for instance, the purification of copper by electroplating, and the deposition of silicon and enriched uranium by a CVD-like process after gas phase processing. Deposition techniques fall in to two categories depending on whether they fall in to chemical or physical (Franscombe and Vossen, 2011)

2.2.1 CHEMICAL DEPOSITION

Here a liquid precursor undergoes a chemical change at a solid layer. Since the fluid surrounds the solid object, deposition occur on every surface, with little regard to direction; thin film from

chemical deposition tend to be conformal rather than directional (Sheshan, 2011). Chemical deposition is further categorized by the phase of the precursor.

2.2.2 PLATING

Plating relies on liquid precursors often a solution of water with salt of the metal to be deposited

2.2.3 SPIN COATING

Spin coating or spin casting uses a liquid precursor or sol-gel precursor deposited on to a smooth, flat substrate which is subsequently spun at a high velocity to centrifugally spread the solution over the substrate. The speed at which the solution is spun and the viscosity determines the ultimate thickness of the deposited film Repeated depositions can be carried out to increase the thickness of films as desired. Thermal treatment is often carried out in order to crystallize the amorphous spin coated films. Such crystalline films can exhibit certain prepared orientations after crystallization on single crystal substrate (Hanoar, *et al.,*2011)

2.2.4 CHEMICAL VAPOR DEPOSITION (CVD)

Chemical vapor deposition generally uses a gas phase precursor, often a halide or hydride of the element to be deposited.

2.2.5 PLASMA ENHANCED (PED)

Uses an ionized vapor or plasma as a precursor. It relies on electromagnetic means (electric current microwave excitation), rather than a chemical reaction to produce plasma.

2.2.6 ATOMIC LAYER DEPOSITION (ALD)

Uses gaseous precursor to deposit conformal thin films one layer at a time The process is split up in two half reactions, run in sequence and repeated for each layer, in order to ensure total layer saturation before beginning the next layer. Therefore one reactant is deposited first and the second reactant, during which a chemical reaction occurs on the substrate forming the desired composition (Hanoar, *et al*., 2011)

2.2.7 CHEMICAL SOLUTION DEPOSITION

A technique for depositing thin film by dipping or spraying a substrate with solution, uses a liquid precursor, usually a solution of organometallic powders dissolved in an organic solvent able of producing stoichiometrically accurate crystalline phases. This technique is also known as sol-gel method because the sol (solution) gradually evolves towards the formation of a gel-like diphasic (Hanoar, *et al.,* 2011).

In this work the chemical solution deposition or sol-gel method is employed to deposit a $CuAlO_2$ thin film on glass substrate because of its cost effectiveness

2.3 OPTICAL PROPERTIES OF THIN FILM

The optical properties of a thin film is the response of the film sample used on the basis of reflectivity, transmissivity and polarization of an incident light which are determined by the distribution index of refraction (n) and extinction coefficient (k). The optical properties are determined from the electromagnetic theory of light as a function of complex refractive index in the case of an absorbing film (Hartnagel, 1995).

UV-Vis refers to absorption spectroscopy in the ultraviolet visiblespectral region, this means it uses light in the visible and adjacent (near-UV andnear-infrared (NIR)) ranges. A sample in a cuvette is exposed to light energy between 190nm and 1000nm. Spectrophotometry investigates the absorption of the lightbetween the wavelength limits 190 nm and 780 nm (visible spectroscopy is restricted to thewavelength range of electromagnetic radiation detectable by the human eye, that is above ~360 nm; ultraviolet spectroscopy is used for shorter wavelengths). In this wavelength rangethe absorption of the electromagnetic radiation is caused by the excitation (i.e. transition to ahigher energy level) of the bonding and non-bonding electrons of the ions or molecules. A micrograph of absorbance against wavelength gives the sample's absorption spectrum. Modernspectrophotometers draw this automatically. The measured spectrum is continuous, due tothe fact that the different vibration and rotation states of the molecules make the absorption band wider. Certain parts of an organic molecule will absorb some of this energy to createpeaks on a spectrum for quantitative (primarily) and qualitative Analysis.(Mardare, *et al.*, *2000*)

The measurement of reflectance of light can be analyzed via the Forouhi Bloomer dispersion equation to determine the index of refraction (n) and the extinction coefficient (k) of a given film across the measured spectral range (Horie, *et al*., 1994).The method is most often in a qualitative way to determine the concentration of an absorbed specimen using Beer Lambert law.

$$A = \log\frac{Io}{I} = \varepsilon cl \qquad 2.1$$

A is the measured absorbance

I_o is the intensity of the incident light at a given wavelength

I is a transmitted intensity

L the path length through the sample and

c the concentration of absorbing specie

ε is a constant known as the molar absorptivity or extinction coefficient with unit1/M cm

The optical band is related to the absorption coefficient using Tauc's relation by,

$$(\alpha hv) = A\,(hv\text{-}E_g)^n \qquad 2.2$$

Where, α is the absorption coefficient

A is a constant (independent from v) and

n the exponent that depend on the kind of optical transmission (n=1/2, 2 when the transition is direct allowed, indirect allowed respectively)

and the photon energy can be calculated using

$$E = hv = \frac{hc}{\lambda} \qquad 2.3$$

this method was depicted by (Lan, *et al.,* 2009).

2.4 ABSORBANCE

The ratio of radiant power (P) transmitted by a sample to the radiant power incident (p_o) on the sample is called the transmittance

$$T = \frac{p}{p_o} \qquad 2.4$$

Absorbance (A) then, is defined as the logarithm (base 10) of the reciprocal of the transmittance

$$A = \log\left(\frac{1}{T}\right) \qquad 2.5$$

In a spectrophotometer, monochromatic plane parallel light enters a sample at right angle to the plane surface of the sample. In this condition the transmittance and absorbance of a sample depends on the molar concentration (c), light path length in centimeters (L) and molar absorption (ε) for the dissolved substances

$$T = 10^{\varepsilon CL} \text{ or } \quad A_\lambda = \varepsilon cL \qquad 2.6$$

Beer's law states that molar absorptivity is constant and absorbance is proportional to concentration for a given substance dissolved in a given solute and measured at a given wavelength (Weast, 1975). Since transmittance and absorbance are unit less, the units for molar absorptivity must cancel with units of measure in concentration and light path. Accordingly molar absorptivity have unit of $M^{-1}cm^{-1}$. Standard laboratory spectrophotometer are fitted for use with 1cm width sample cuvettes, hence the path length (L) is generally assumed to be equal to one and the term is dropped altogether in most calculations so that

$$A_\lambda = \varepsilon\, c\, L = \varepsilon\, c \qquad 2.7$$

where, L=1cm

2.5 THE ABSORPTION COEFFICIENT

The absorption coefficient determines how far into a material light of a particular wavelength can penetrate before it is absorbed. In a material with low absorption coefficient, light is only poorly absorbed, and if the material is thin enough, it will appear transparent at allwavelengths. The absorption coefficient depends on the material and also on the wavelength of light which is being absorbed. Semiconductor materials have a sharp edge in the absorption coefficient, since light which has energy below the band gap does not have sufficient energy to excite an electron in to the conduction band from the balance band, consequently this light is not absorbed. (Christiana, *et al.,* 2006).The absorption coefficient for several semiconductor materials is shown in fig.2.1 below

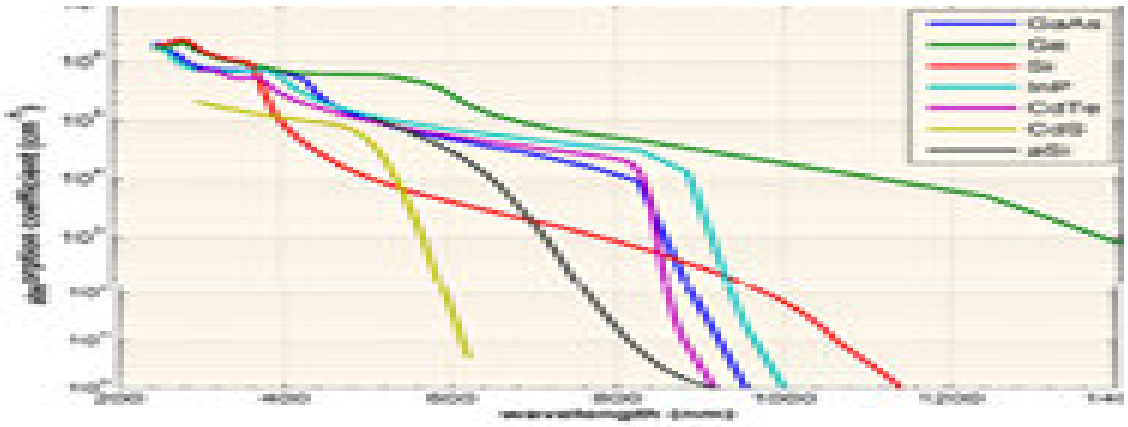

Fig. 2.1 Absorption coefficient vs wavelength for semiconductor materials (Christiana and Staurt, 2003)

2.6 FOURIER TRANSFORM INFRARED (FT-IR) SPECTROSCOPY

Fourier transform infrared spectroscopy is an analytical technique used to identify organic (and in some cases inorganic) materials. The technique measures the absorption of radiation by the sample material versus wavelength. The infrared absorption bands identify molecular components and structures. (Griffiths and Hasseth, 2007). The FT-IR measures the range of wavelengths in the infrared region that are absorbed by a material. This is accomplished through the application of infrared radiation (IR) to samples of a material. When this IR radiation is passed through the sample, some of the infrared radiation is absorbed by the sample and some is passed through (transmitted). The resulting spectrum represents the molecular absorption and transmission creating a molecular finger print of the sample (Brault, 1996).This makes infrared spectroscopy useful and more advanced than several types of analysis because the following advantages:

i-It can identify unknown materials

ii-It can determine the quality or consistency of the sample

iii-It can determine the amount of components in the mixture

iv-It is a non-destructive technique

v- It provides precise measurement method which requires no external calibration

vi- It has greater optical thorough put

vii- It is mechanically simple with only one moving part

vii- It has greater speed because all of the frequencies are measured simultaneously.

viii- FT-IR detectors are much more sensitive, because the optical throughput is much higher which results in much lower noise level, and the fast scans enable the co-addition of several scans in order to reduce the random measurement noise to any desired level (Brault, 1996)

CHAPTER THREE

3.0 MATERIALS AND METHOD

3.1 MATERIALS

SALTS:

Cuprous chloride (CuCl 99.9% purity Loba India)

Aluminium Chloride ($AlCl_3$ 99.9% purity Mark)

Sodium hydroxide pellets (NaOH Loba)

LIQUIDS:

Concentrated hydrochloric acid HCl

Distilled water

Deionized water

Acetone

Soap solution

SUBSTRATE: Five ordinary microscopic glass slides as Substrate

3.2 METHOD

3.2.1 SOL-PREPARATION

A sol was prepared by adding concentrated hydrochloric acid, to cuprous chloride (CuCl) powder and the solution was stirred using a magnetic stirrer. During this stirring process further addition of hydrochloric acid to the solution was done until all the salts were dissolved in it.

Another solution was also prepared by adding distilled water drop by drop to Aluminium chloride ($AlCl_3$) salts to dissolve it completely.

The two solutions were mixed together and some excess distilled water added to the mixture. The solution was further stirred at an elevated temperature of 80^{o}c for 2hours. Now during this stirring process, some amount of sodium hydroxide pellets was added to the solution to control the pH value to around 2 (acidic medium) this makes the mixed solution appeared darker and gel like. The solution was then aged for 3 hours so as to get the required sol which was used for the dipping process in the second stage.

3.2.2 SUBSTRATE PREPARATION

Five ordinary microscopic slides were used as substrates, the choice of which is because it is transparent, flat, thin enough and also able to adequately adhere the Cu-Al films to it; not only at normal temperature but also during relatively large temperature changes during the annealing process.

Before the dipping process these glass substrates were cleaned with mild soap solution, then washed thoroughly in deionized water and also in boiling water. Finally they were ultrasonically cleaned in acetone for 20 minutes

3.3 COATING PROCESS

During this process, the substrates were completely dipped one by one in to the jelly sol and withdrawn vertically slowly at a rate of 10cm /min for 8 times. Between two successive dipping, the substrate along with the carried sol were dried at a temperature 100-120^{o}C so as to have a quick gelation. After the dipping and withdrawing procedure, the resulting five $CuAlO_2$thin film samples were now ready for annealing.

3.4 ANNEALING PROCESS

Four of the five samples of $CuAlO_2$ thin films deposited using the sol-gel technique were annealed at temperatures of 400ºC, 500ºC, 600ºC and 700ºC for 2hrs each and the annealed thin films are kept ready for structural and optical analysis.

3.5 STUDY OF THE SURFACE MORPHOLOGY

This study was carried out on all the five samples (as-synthesized and annealed) samples of thin films of $CuAlO_2$ using the SEM Hitachi S-1100Model scanning electron microscope.

3.5.1 THE SEM MEASUREMENTS

The scanning electron microscope (SEM) produces images of a sample by scanning the sample surface with a focused beam of electrons; the electrons interact with atoms in the sample, producing various signals that can be detected and contain information about the samples' surface topography and composition. The electron beam generally scanned in a raster scan pattern and the beams position combined with the detected signal to produce an image to achieve resolution better than 1nm. The process was conducted in high vacuum and at a wide range cryogenic or elevated temperatures. The most common SEM mode is the detection of secondary electrons emitted by atoms excited by the electron beams. The number of secondary electrons that can be detected defends on the energy at which the beam meets the surface of specimen (McMullan, 2006). By scanning the sample and collecting the secondary electrons with a special detector an image displaying the topography of the surface is created

Plate 3.1. Hitachi S-4100 Scanning Electron Microscope(SEM) (at UMYU, Katsina)

3.5.2 SEM COMPONENTS AND OPERATION

The scanning electron microscope (SEM) consists of an energetically well-defined highly focused beam of electrons scanned across a sample. The microscope uses a LaB6 source and is pumped using turbo and ion pumps to maintain the highest possible vacuum. (Klein,2012) A finely focused electron beam scanned across the surface of the sample generates secondary electrons backscattered electrons, and characteristic x-rays. These signals are collected by detectors to form images of the sample displayed on a cathode ray tube screen. Secondary electron imaging (SEI) works on the principle that this electron beam generates a 'splash' of electrons with kinetic energy much lower than the primary incident electrons called secondary electrons. Because of their low energies and low penetration depth, the detection of secondary electrons as a function of primary beam position makes it possible to attain high magnifications (as much as x100, 000 in some cases) and high resolutions (up to~40A solution). For imaging the

areas of interest, backscattered imaging (BEI) detects high energy electrons which backscatter quasi-elastically of the sample.

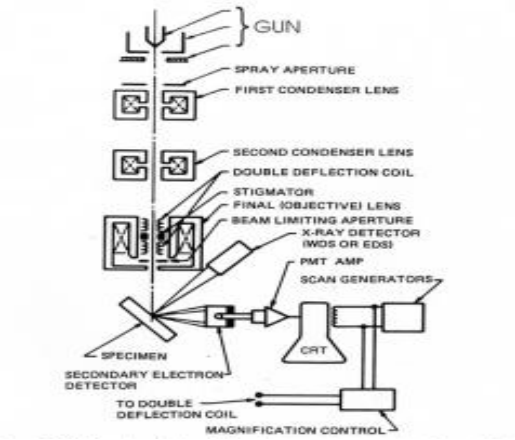

Fig. 3.1 Schematic diagram of SEM

This imaging detector operates in two modes: Topographical, which yields a topographic image of the sample surface; and compositional, which distinguishes between areas of relative low and high average atomic weights. This techniqueis extremely useful for locating areas with concentrations of heavy elements not necessarily visible to the naked eye or to the secondary electron detector.

3.5.3 MAGNIFICATION AND IMAGE FORMATION

SEM can be controlled over a range of up to 6 orders of magnitude from 10 to 500,000 times. Unlike optical transmission electron microscope, image magnification in SEM is not a function of the objective lens. SEMs may have condenser and objective lenses, but their function is to focus the beam to spot, and not to image the specimen. Magnification results from the ratio of the dimensions of the raster on the specimen and

the raster on the display device. Magnification is therefore controlled by current supplied to the x,y scanning coils or the voltage supplied to the x,y deflection plates and not by objective lens power.

3.5.4 SAMPLES PREPARATION FOR SEM MEASUREMENTS

Fourout of the five annealed samples were cut and made appropriate sizes of one square centimeter each to fit in to the specimen chamber and were generally mounted rigidly on a specimen holder called a specimen stub. To prevent scanning faults the specimens were completely dried since the specimen chamber is at high vacuum the images were then displayed on a screen for observations

3.6 STUDY OF THE OPTICAL CHARACTERISTICS

This study was carried out in two stages

i-By UV-Visible spectrophotometry and

ii-By Fourier Transform Infrared FT-IR

The purpose of which is to determine the properties exhibited by the $CuAlO_2$thin film in the presence of light and annealed at a temperature range of 400-700^oC in the intervals of 100^oC each. The optical and solid state properties studied include Transmittance (T),Absorbance (A) Absorption coefficient (α), extinction coefficient (k) and the band gap

3.7 UV-VISIBLE SPECTROPHOTOMETER

The UV-visible spectrophotometer used for this work is Varian Cary 50Bio

UV-Vis spectrophotometer fig.3.3 below

Plate. 3.2 Varian Cary 50Bio model uv 0906M012 uv-visible spectrophotometer (at Dept. Of Biochemistry B.U.K)

3.7.1 THE WORKING PRINCIPLE OF UV-VIS SPECTROPHOTOMETER

It uses light in the visible range and adjacent (near UV-and near infrared (NIR) ranges). The absorption or reflectance in the visible range directly affects the perceived color of the chemicals involved. In this region of the electromagnetic spectrum, molecules undergo electronic transition. This technique is complementary to fluorescence spectroscopy. Molecules containing π-electrons or non-bonding electrons (n-electrons) can absorb the energy in the form of ultraviolet or visible light to excite these electrons to higher anti-bonding molecular orbitals, (Misra and Dubinskii, 2002). UV-Vis spectroscopy in this semiconductor measures the thickness and optical properties of the thin film on glass, fig. 3.3

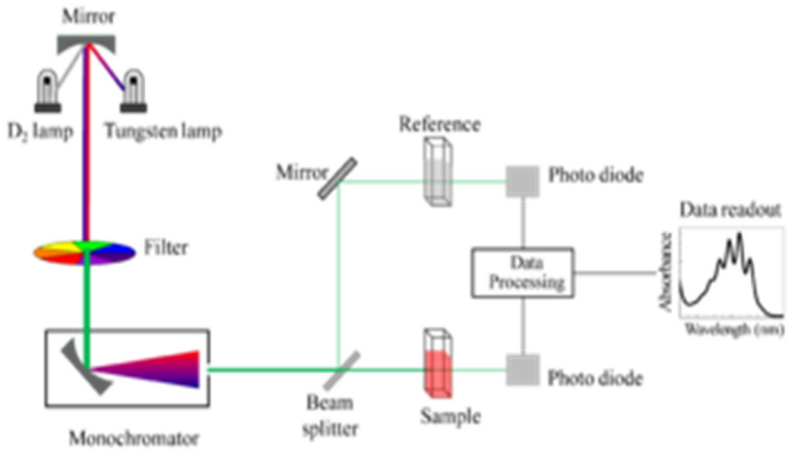

fig.3.3 Scheme diagram of a UV- Vis spectrophotometer

3.7.2 SAMPLE PREPARATION FOR UV-MEASUREMENTS

Samples for UV-Vis spectrophotometry using the Varian Cary 50 Bio mode are most often liquids, and typically placed in a transparent cell, known as cuvette. The cuvette is typically rectangular in shape commonly with an internal width of 1cm, this width become the path length L in the Beer Lambert law. It allows radiation to pass over the spectral region of interest. The most widely applicable cuvette is made of high quality fused silica or quartz glass because they are transparent throughout the UV-visible and near infrared regions (Skoog *et al*., 2007)

In this work small portions of all the six samples of the prepared $CuAlO_2$ thin films were scrapped and the powder diluted with distilled water and placed in to separate cuvettes for UV-Vis spectrophotometry

3.8 FOURIER TRANSFORM INFRARED (FT-IR) SPECTROSCOPY

Fourier transform infrared spectroscopy is an analytical technique used to identify organic (and in some cases inorganic) materials. The technique measures the absorption of radiation by the sample material versuswavelength. The infrared absorption bands identify molecular components and structures.

3.8.1 COMPONENTS PRINCIPLES AND MEASUREMENT OF FT-IR SPECTROMETER

The material or specimen placed is irradiated with infrared radiation. Absorbed IR radiation usually excites molecules into a higher vibrational state. The wavelength of light absorbed by a particle molecule is a function of the energy difference between its rest and excited vibrational states. The wavelengths that are absorbed by the sample are characteristics of molecular structure (Nishikida, *etal.,*1995) The FT-IR spectrometer uses an interferometer fig.3.5 to modulate the wavelength from broadband infrared source. A detector measures the intensity of transmitted or reflected light as a functionof its wavelength.

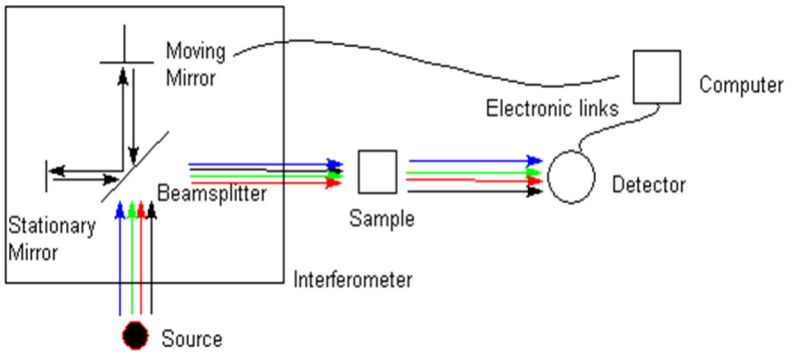

fig 3.4 schematic diagram of FT-IR

The signal obtained from the detection is an interferogram, which must be analyzed with a computer using Fourier transform to obtain a single-beam infrared spectrum. The FT-IR spectra are presented as plots of intensity versus wave number (cm^{-1}). Wave number is the reciprocal of wavelength. The intensity is plotted as a percentage of light transmittance or absorbance or reflectance at each wave number as in fig.3.6

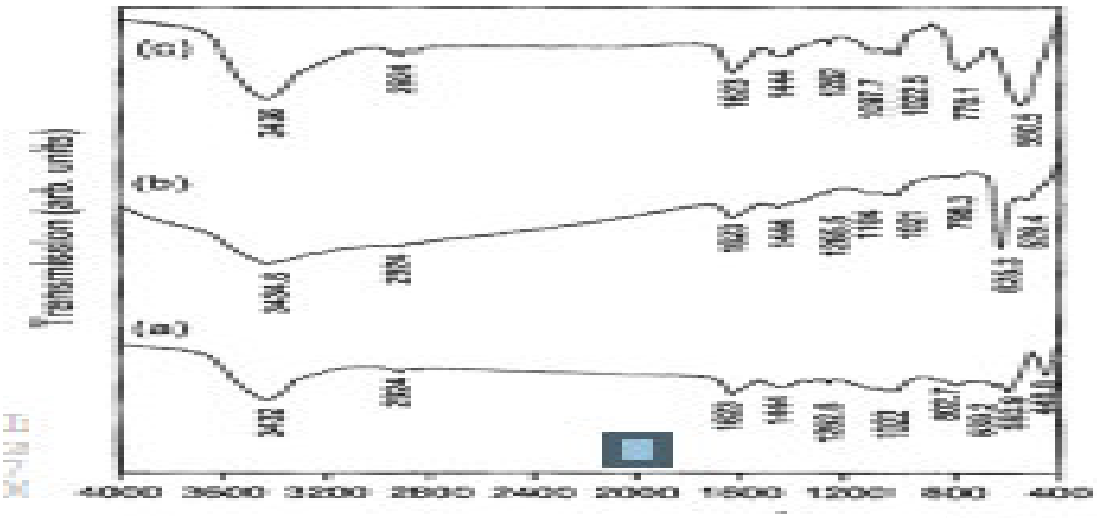

Fig.3.5 FT-IR spectra for (a) $CuAlO_2$, (b) Cu_2O and (d) α-Al_2O_3 (Prakash, *et al., 2008*)

3.8.2 SAMPLE PREPARATION FOR FT-IR SPECTROMETER MEASUREMENT

Small portion of all the four coated and annealed samples of $CuAlO_2$ thin film were scrapped using a sterile blade to obtain the powdered samples, these were placed on FT-IR spectrometer stage for FT-IR analysis

CHAPTER FOUR

4.0 RESULT AND DISCUSSION

Plates 4.1 to 4.5 show the SEM micrographs of the as synthesized and annealed samples of the deposited $CuAlO_2$ thin film on glass substrate using the chemical solution (sol gel) method of deposition. From the micrograph of Plate 4.1 (as deposited $CuAlO_2$ sample) it will be observed that the film had loose structure with small particle size and a fine and well define grain boundaries and size, the grain size appears smaller compared with those annealed at different temperatures, also the film color is black and uniformly covering the substrate with good adherence.

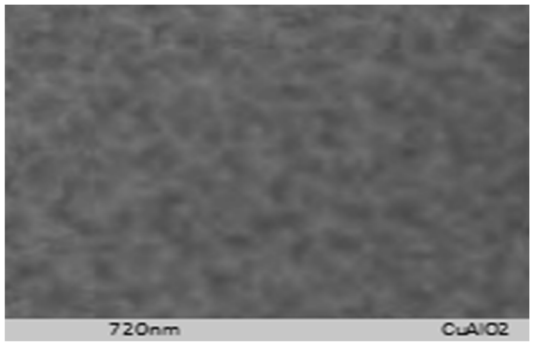

Plate 4.1 SEM micrograph of as synthesized $CuAlO_2$

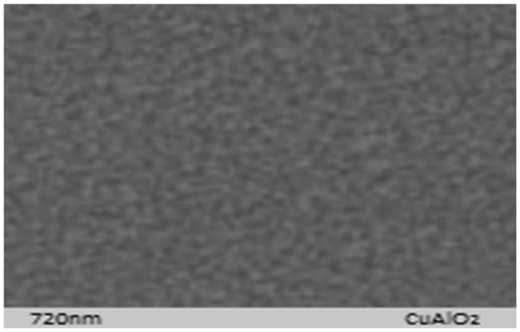

Plate 4.2 SEM micrograph of $CuAlO_2$ annealed at 400°C

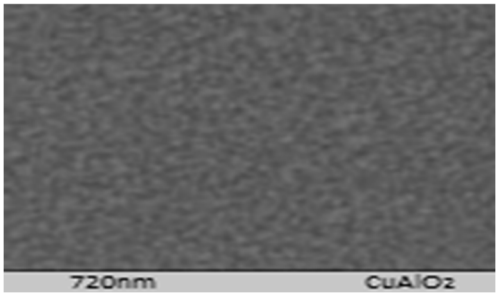

Plate 4.3 SEM micrograph of $CuAlO_2$ thin film annealed at 500°C

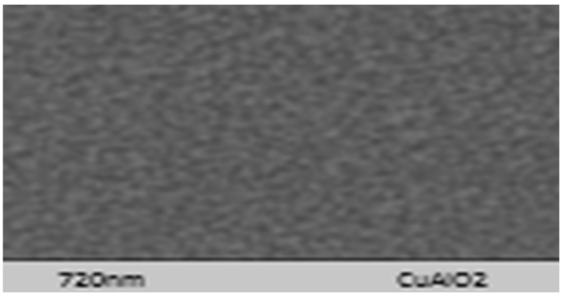

Plate 4.4 SEM micrograph of $CuAlO_2$ thin film annealed at 600°C

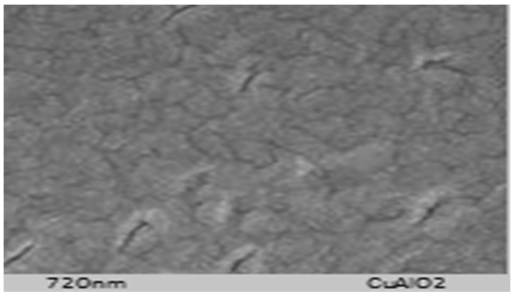

Plate 4.5 SEM micrograph of $CuAlO_2$ thin film annealed at 700°C

The micrographs of Plates 4.2 to 4.5 showed a similar structure with larger particles size and at these temperatures the film look more compact there is the existence of a smooth surface with finer grain. Again some bigger clusters are also shown to be dispersed on the surface which resulted due to agglomeration of finer grains. It is apparent that the grain size of the films increases as the annealing temperature increases which can be understood by high mobility of atoms at high annealing temperatures. This result agrees with the work of (Wang, 2003) who found a similar results of the structure of Cu-Al-O film deposited at a temperature of 750^{o}C with lager particle size of about 40-50nm. Dense granular structures are also observed in the images with some voids visible at the middle of the structure this agrees with the work of (Lan, *et al.,* 2009). It is also worth to notice that the micrographs of Plate 4a, and 4b are having similar type of crystallinity due to the annealing temperature range of 400^{o}C and 500^{o}C, it now appears that due to the annealing temperatures of the micrographs of Plates 4.1 and 4.2, the densification of the films has not fully taken place. However a further elevated thermal treatment as in micrographs of Plates 4.4 and 4.5 reduces the voids in the micrographs. It is also to be observed that the overall surface of the micrograph of Plate 4.5 is seen to have finer grain boundaries covering the substrate which is attributed to the elevated thermal treatment of 700°C.

4.1 STUDY OF THE OPTICAL PROPERTIES

Optical properties of $CuAlO_2$ thin film are extremely important because of its possible applications in the field of optoelectronics technology. High transparency is one of the main features of TCOs. Therefore detailed optical characterization and determination of related parameters are the most significant part of the analysis of TCOs. Following this point of view, the optical properties of $CuAlO_2$ thin films in terms of absorbance, transmittance, absorption coefficient, extinction coefficient and band gaps have been studied in detail. The four samples S1, S2, S3 and S4 of the deposited $CuAlO_2$ film with different annealing temperatures of 400°C, 500°C, 600°C and 700°C respectively with 2hrs annealing time each were studied and analyzed.

Table 4.1 Showing wavelength, absorbance and transmittance for sample1 (S1) annealed at 400°C

S/N	Wavelength (nm)	Absorbance	% Transmittance
1	325	0.525	18.70
2	350	0.456	35.00
3	370	0.460	36.00
4	390	0.430	38.70
5	400	0.456	39.20
6	450	0.460	40.00
7	500	0.470	42.00
8	550	0.475	42.20
9	570	0.476	42.25
10	600	0.480	42.10
11	650	0.488	42.91
12	660	0.490	42.91
13	700	0.493	42.90
14	725	0.494	42.95
15	750	0.500	42.96
16	800	0.500	43.60
17	850	0.498	43.90

Table 4.2 Showing wavelength, absorbance and Transmittance for sample 2 (S2) annealed at 500˚C

S/N	Wavelength (nm)	Absorbance	% Transmittance
1	325	0.655	18.7
2	350	0.575	54.2
3	370	0.564	56.0
4	390	0.570	56.6
5	400	0.565	57.6
6	450	0.565	58.9
7	500	0.550	59.5
8	550	0.540	60.0
9	570	0.530	60.0
10	600	0.525	60.1
11	650	0.526	60.1
12	660	0.532	60.0
13	700	0.524	60.1
14	725	0.525	60.0
15	750	0.515	60.0
16	800	0.530	59.6
17	850	0.510	59.4

TABLE 4.3 Showing wavelength, absorbance and reflectance for sample 3 (S3) annealed at 600ºc

S/N	Wavelength (nm)	Absorbance	% Transmittance
1	325	0.855	18.7
2	350	0.650	62.5
3	370	0.640	62.9
4	390	0.630	63.0
5	400	0.625	64.0
6	450	0.620	64.1
7	500	0.610	67.0
8	550	0.600	70.0
9	570	0.600	70.5
10	600	0.600	71.1
11	650	0.610	72.0
12	660	0.618	72.0
13	700	0.610	71.3
14	725	0.609	71.9
15	750	0.610	72.1
16	800	0.616	72.5
17	850	0.610	72.9

Table 4.4 Showing wavelength, absorbance and transmittance for sample 4 (S4) annealed at 700°C

S/N	Wavelength (nm)	Absorbance	% Transmittance
1	325	0.855	18.7
2	350	0.650	62.5
3	370	0.640	62.9
4	390	0.630	63.0
5	400	0.625	64.0
6	450	0.620	64.1
7	500	0.610	67.0
8	550	0.600	70.0
9	570	0.600	70.5
10	600	0.600	71.1
11	650	0.610	72.0
12	660	0.618	72.0
13	700	0.610	71.3
14	725	0.609	71.9
15	750	0.610	72.1
16	800	0.616	72.5
17	850	0.610	72.9

Table 4.5 showing wavelength, absorbance, absorption coefficient extinction coefficient and energy for samples S1 and S2

S/N	Wavelength (nm)	% Absorbance (A)		Absorption coefficient (α x $10^6 m^{-1}$)		Extinction coefficient (k x 10^{-3})		$E=\frac{hc}{\lambda}$ (ev)	$(\alpha E)^2$ X 10^{13} $(eVm^{-1})^2$	
		S1	S2	S1	S2	S1	S2		S1	S2
1	300	1.400	1.400	4.478	4.478	106.9	106.9	4.13	34.20	34.20
2	325	0.525	0.655	1.679	2.095	43.40	54.10	3.81	4.10	6.39
3	350	0.456	0.575	1.459	1.839	40.60	51.20	3.54	2.67	4.24
4	370	0.460	0.574	1.471	1.836	43.30	54.10	3.35	2.43	3.78
5	390	0.430	0.570	1.375	1.823	42.60	56.60	3.18	1.91	3.36
6	400	0.456	0.565	1.459	1.807	46.70	57.50	3.10	2.04	3.14
7	450	0.460	0.565	1.471	1.807	52.70	64.70	2.76	1.64	2.48
8	500	0.470	0.550	1.503	1.759	59.80	69.90	2.48	1.39	1.90
9	550	0.475	0.540	1.519	1.727	66.50	75.60	2.25	1.29	1.52
10	570	0.476	0.530	1.523	1.695	69.10	76.90	2.18	1.17	1.36
11	600	0.480	0.525	1.535	1.679	73.30	80.20	2.07	1.10	1.20
12	650	0.488	0.526	1.561	1.682	80.70	87.10	1.91	1.01	1.03
13	660	0.490	0.532	1.567	1.673	82.30	87.90	1.88	0.82	0.94
14	700	0.493	0.524	1.577	1.676	87.90	93.40	1.77	0.78	0.88
15	725	0.494	0.525	1.580	1.679	91.20	96.90	1.71	0.73	0.82
16	750	0.500	0.515	1.599	1.647	95.40	98.30	1.65	0.61	0.74
17	800	0.500	0.530	1.599	1.695	101.8	107.9	1.55	0.61	0.69

0.81au, 0.63au, 0.52au and 0.45au for samples S1, S2, S3and S4 respectively in the wavelength region of about 400nm.

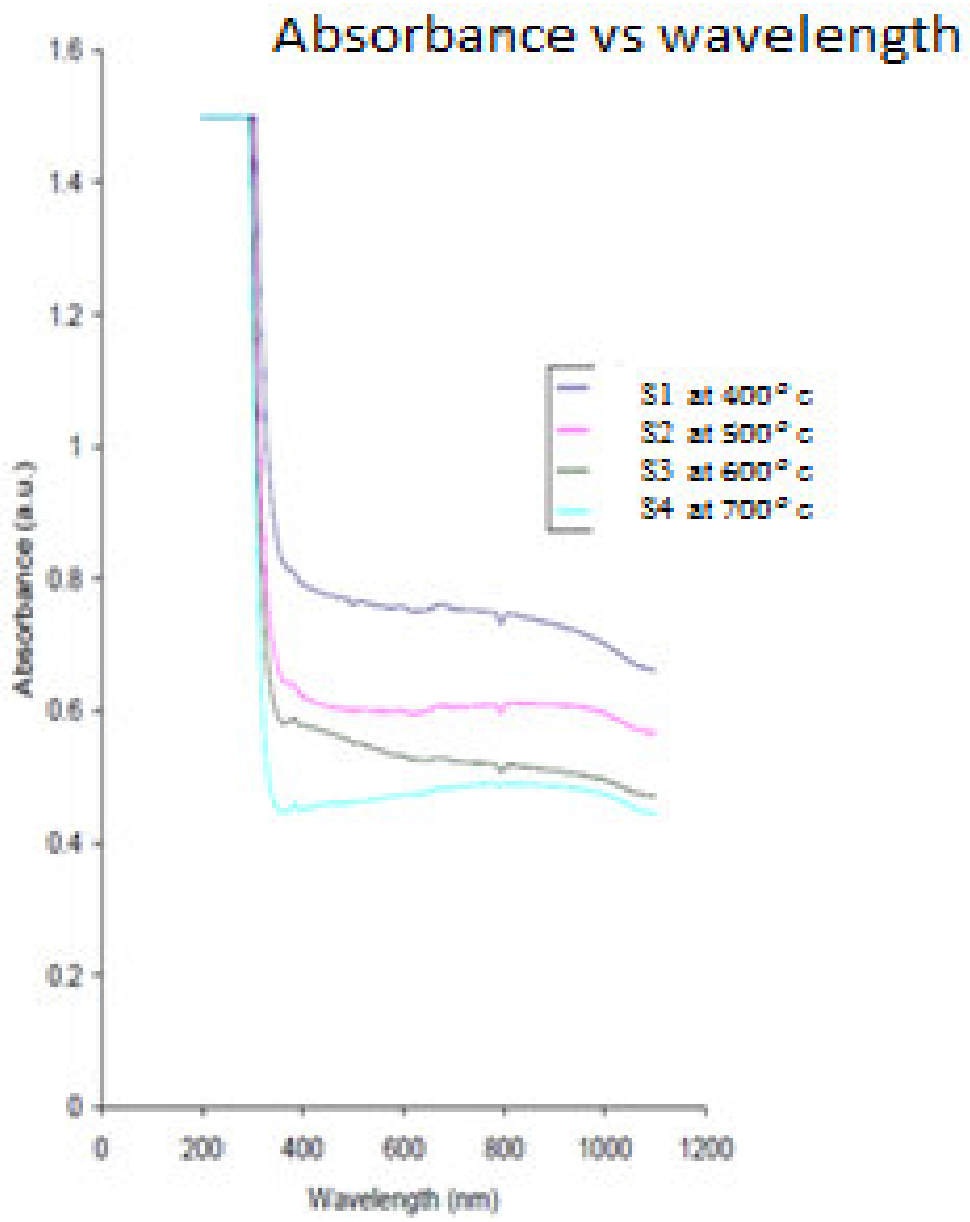

Fig.4.6a Absorbance vs wavelength spectra for $CuAlO_2$ thin film at different annealing temperatures

Within the visible range the absorbance value of some of the samples decrease from about 0.81au to 0.75au, 0.63au to 0.62au and 0.59au t00.52au for samples S1, S2 and S3 respectively. However the absorbance of sample S4 increases slowly from about 0.45au to about 0.48au within the visible range. Between 700nm and 900nm, the absorbance values of the samples are fairly constant. While the absorbance values of samples S1 and S2 are about 0.75au and 0.62 within this range the value for samples S3 and S4are about 0.52au and 0.45au respectively. Beyond 900nm, absorbance value of all samples decreases slowly with increase in wavelength.

4.1.2 TRANSMITTANCE FOR THE SAMPLES

The transmittance of the samples increases with increasing annealing temperature. It rises from a common value of about 18.3% at about 306nm to peak values of about 38.6%, 54.3%, 62.3%, and 86.1% in the infrared region and a small decrease occurs around 400nm in all the samples. Between 400nm and 700nm the transmittances of the samples S1, S2, S3 and S4 rise from 37.53% to 42.5%, 53.2% to 54.00% and 85.32% to 87.61% respectively and this agrees with the work of (Mammah, *et al*., 2005).

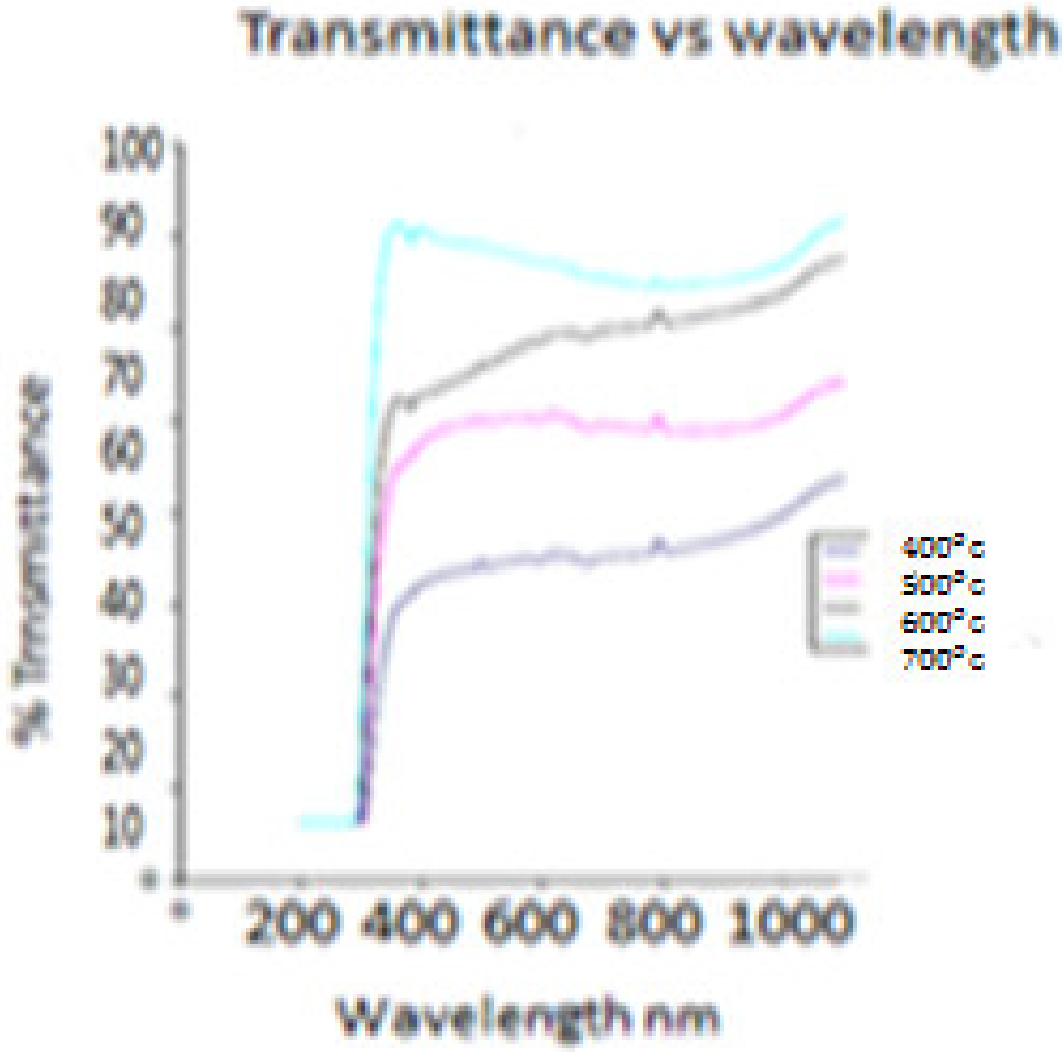

Fig.4.6b Transmittance vs wavelength spectra for $CuAlO_2$ thin film at different annealing temperatures

4.1.3 ABSORPTION COEFFICIENT

The absorption coefficients (α) are calculated from the absorbance data using the Beer Lambert equation given as (Lambert, 2006)

$$\alpha = \frac{2.203A}{d} \qquad 4.1$$

Where,

A is the absorbance and

d is the thickness of the film

The absorption coefficient α decreases with increasing annealing temperature. The absorption coefficient of three samples S1, S2 and S3 increases according to fig4.1d from 1.58×10^{-6}, 1.29×10^{-6} and 1.08×10^{-6} at about 1.14ev in the infrared region to about 1.93×10^{-6} , 1.58×10^{-6} and 1.29×10^{-6} at about 3.62eV in the visible region and this agrees with the work of (Kim *et al*., 2007). And between 3.62eV and 4.00eV, the absorption coefficient of the samples rises sharply and attained different peak values which decreases with increasing annealing temperature.

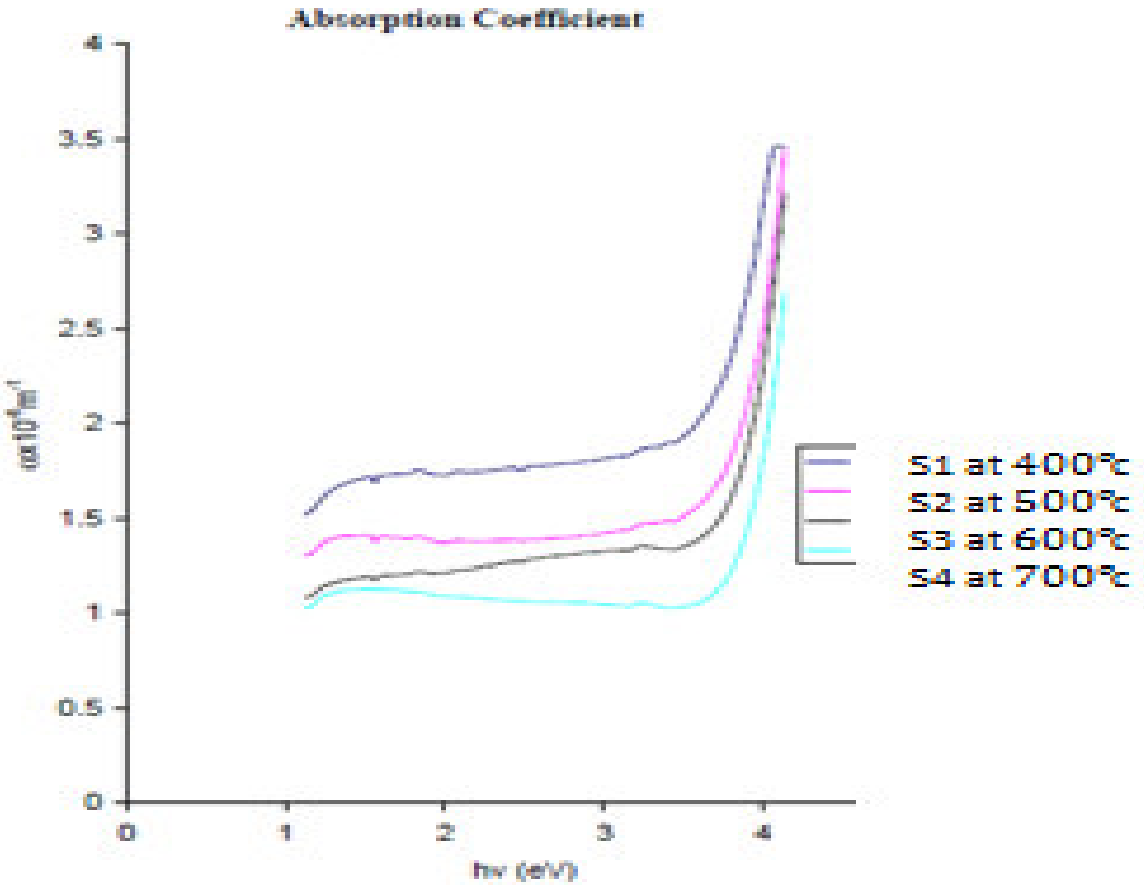

Fig. 4.6 c absorption coefficient vs photon energy for $CuAl_2O$ thin film at different annealing temps**.**

4.1.4 ENERGY BAND GAP

The energy in electron volt (eV) is obtained using

$$E = hv = \frac{hc}{\lambda} \qquad 4.2$$

Where, h is a Planck's constant given as 6.62×10^{-34}Js

c is the speed of light

and λ is the wavelength

4.1.5 DIRECT BAND GAP

The direct band gap for all the samples is calculated using Tauc's relation from the values obtained for absorption coefficient ($\boldsymbol{\alpha}$) and energy gap (E). The direct band gap according to the plot in fig 4.2f for sample S1 is about 3.55eV while that of S2 and S3 is about 3.80eV and that of sample S4 has a direct band gap of about 3.85eV. This values agrees with the values of the band gaps estimated by (Lan, *et al*., 2009) as 3.0, 3.15, 3.50 and 3.75 and the work of (Arghya, 2010) who extrapolate the linear portions of the graphs of $(\alpha hv)^{1/n}$ =A(hv-E) to the hv axes and obtained a obtained a direct band gap of $CuAlO_2$

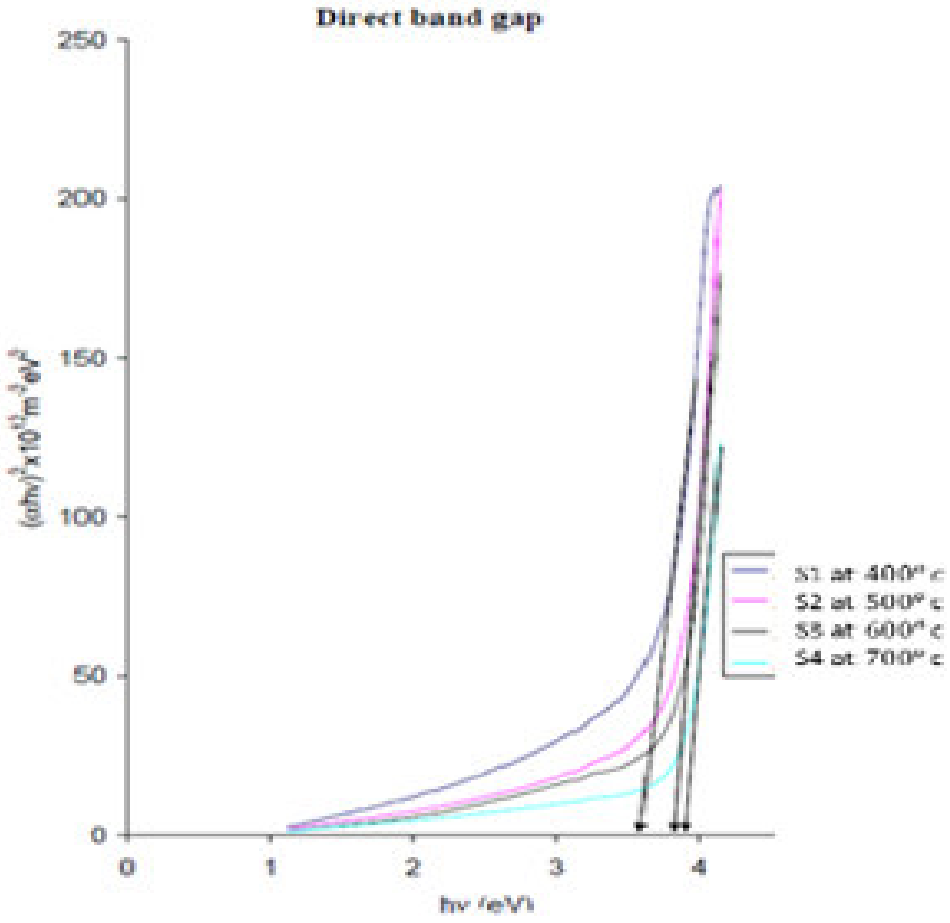

Fig 4.6d Direct band gap vs photon energy for $CuAlO_2$ thin film at different annealing temperatures

4.1.6 THE EXTINCTION COEFFICIENT

The extinction coefficient (k) of all the samples are calculated from the values of absorption coefficient (α) calculated from the equation (Bryce, 2003)

$$k=\frac{\lambda\alpha}{4\pi} \qquad 4.3$$

From the plot of fig.4.1e, the extinction coefficient of the samples S1, S2, S3, and S4 decreases parabolically from 133.89 x 10^{-3}, 111.76 x 10^{-3}, 93.45 x 10^{-3} and 89.44 x 10^{-3} respectively in the infrared region to about 81.11 x10^{-3}, 82.22 x10^{-3}, 83.35x10^{-3} and 84.42x10^{-3} at about 4.05eV in the visible region respectively. The minimum values of the extinction coefficientare 57.78x10^{-3}, 29.44x10^{-3} for samples S2 and S1 respectively and it occurs at about 3.54ev. Now the extinction coefficient values of the samples at 2ev are approximately 94.32x10^{-3}, 72.58x10^{-3}, and 64.44x10^{-3} and 59.46x10^{-3} for samples S1, S2, S3, and S4 respectively and these values are comparable with those in the work of (Arghya, 2010) whose values of the extinction coefficients vary from 22.00x10^{-3} to 65.32x10^{-3} in the wavelength region of 300-800nm

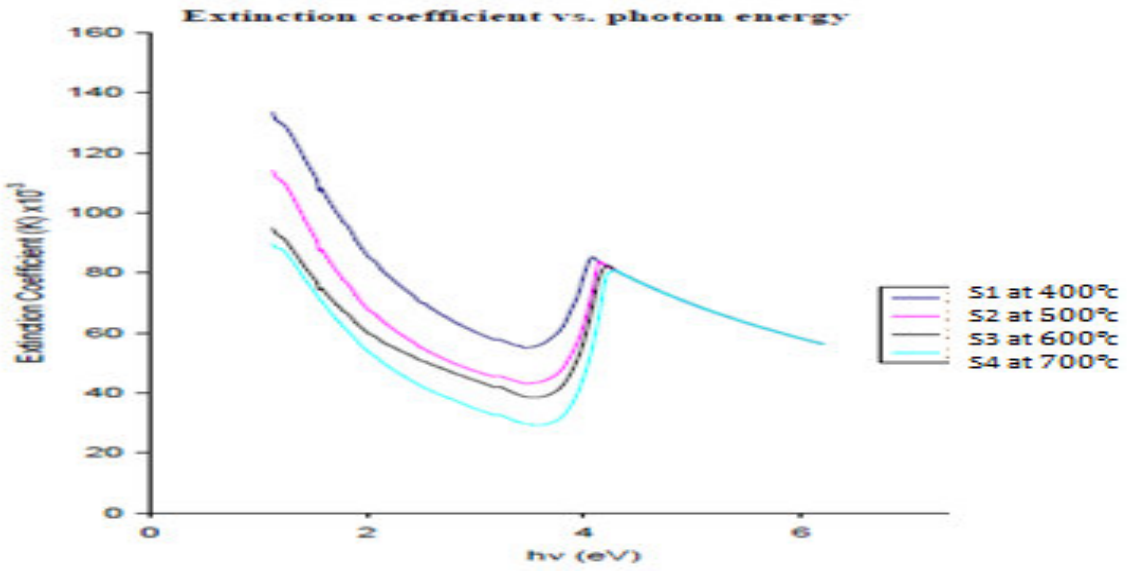

Fig. 4.2e Extinction coefficient vs photon energy of $CuAlO_2$ thin film at different annealing temperatures

4.2 FOURIER TRANSFORM ANALYSIS OF THE CUALO$_2$ THIN FILM

Fourier transform infrared spectroscopy (FT-IR) performed on the $CuAlO_2$ thin film deposited on microscope slide (glass slide) as substrate was only carried out on sample S4 annealed at temperature 700˚C, this is because in the uv-visible spectrophotometry all the samples of the deposited $CuAlO_2$ thin film annealed at 400˚C, 500˚C, 600˚C and 700˚C were analyzed for all parameters and the results were discussed.

4.2.1 ABSORBANCE IN FT-IR SPECTROSCOPY

The absorbance for all the samples annealed at different temperatures decreases with increasing annealing temperature as found in the UV- Visspectrophotometry

of fig.4.2afor this sample S4 annealed at 700˚C, the FT-IR spectra of absorbance vs wavenumber cm^{-1} is given in fig. 4.3a.

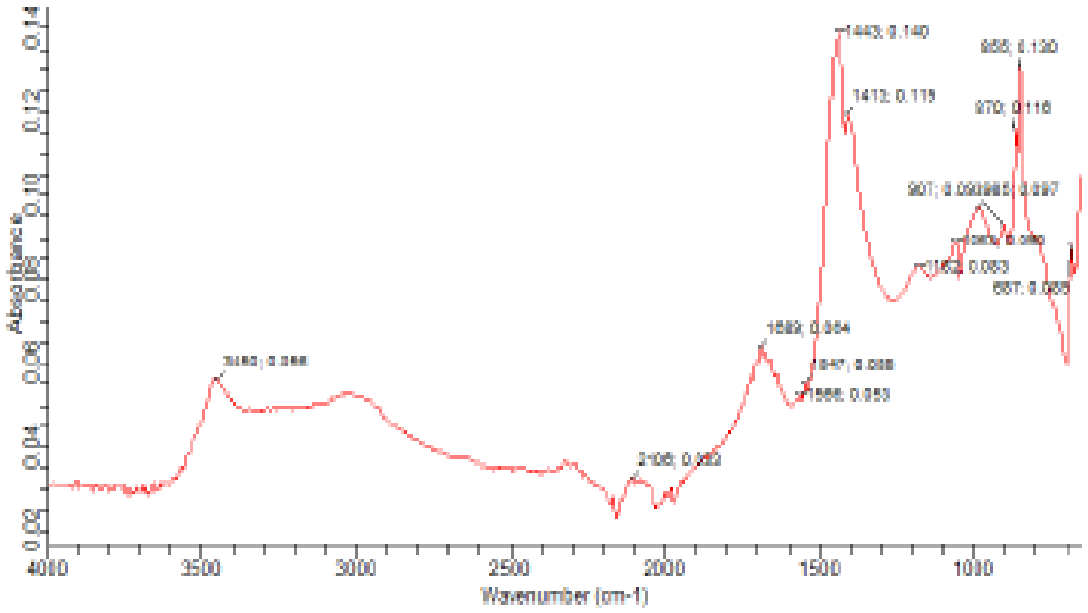

Fig. 4.3a FT-IR Spectra for absorption vs wavenumber cm^{-1} for sample S4 ($CuAlO_2$ thin film) annealed at 700˚C

The wave number varied from 700 to 400cm^{-1}in the spectra, the absorbance decreases with an increase in temperature, the absorbance is at its lowest value of about 0.031au at a wave number of at 2106cm^{-1} and a peak value of 0.14au at a wave number of 1443cm^{-1}. Between the wavenumber of 3600cm^{-1}4000cm^{-1} there is almost no change in the absorbance value of the given sample. However there appears a sudden rise in the absorbance values from 0.031au to 0.055au at a region between 3450cm^{-1} to 3570cm^{-1}m wavenumber. The two highest peaks at 0.140au (1443cm^{-1}) and 0.130au 855cm^{-1} may be attributed to the Al-O and CuO stretching and bending vibration change in surface structure taking place after calcination. And between the wavenumbers of about 1480nm (0.140au) to 1547nm (0.055au) there appears a very sharp decrease in the absorbance of the sample. (Smith, 1999) in his infrared spectral interpretation observes the decrease in his spectra of $CuAl_2O_4$ Nanopowder

4.2.2 TRANSMITTANCE IN FT-IR SPECTROSCOPY

Transmittance generally increases with an increase in the annealing temperature (Mammah, *et al*., 2003) this was also previously reached in the UV-Vis transmittance spectra of all the samples of $CuAlO_2$ produced at different annealing temperatures of fig.2.1 above. For the FT-IR transmittance of the sample annealed at 700°C temperature the spectra of the film is produced in fig.4.3a

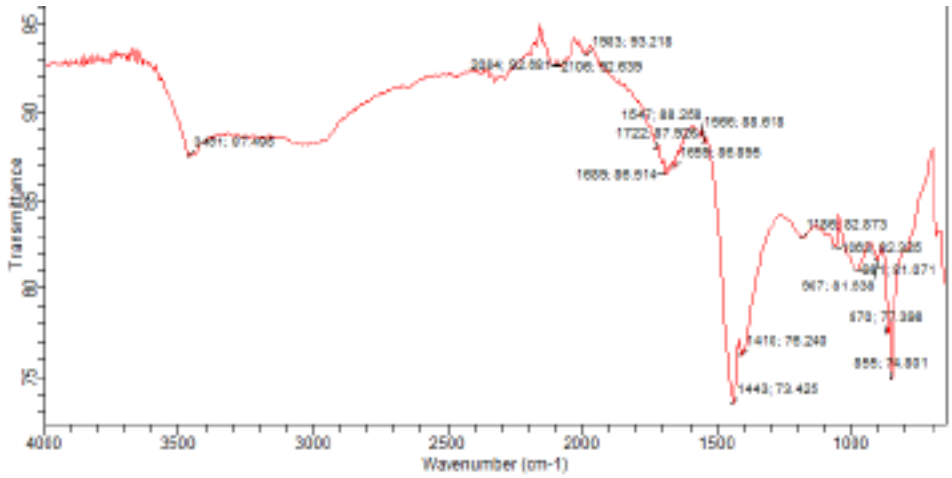

Fig.4.7b FT-IR spectra for transmittance vs wavenumber cm^{-1} for sample S4 ($CuAlO_2$ thin film) annealed at 700˚C

The wave number varies from about 700cm^{-1} to 400cm^{-1} in the above spectra, there appears almost constant transmittances of about 85% and 95% at the wave number regions of about 2980cm^{-1} to 3900cm^{-1} and 3645cm^{-1} to 4000cm^{-1}. The two lowest peaks at the wavenumber region of 700cm^{-1} to 1443cm^{-1} with transmittances of 73.425% and 74.801% may be attributed to Cu-O stretching vibration fig.4.7b. And the other peak at 1185cm^{-1} wavenumber equivalent to 82.873% transmittance may be due short Al-O stretching vibration in distorted AlO_6 octahedra. The peak at 1689cm^{-1} equivalent to 86.51% transmittance may be due to OH stretching vibration which may be incorporated from the atmospheric contaminations, other similar peaks in 2084cm^{-1} equivalent to 92.681% and 1983cm^{-1} equivalent to 93.218% may be attributed to O-Al vibration which occurs due to the nature of the $CuAlO_2$ film in the sample lastly a peak at 3461cm^{-1}(87.495% transmittance) may be a CO_2 peak. This is comparable with the work of (Prakash,*et al.,*2008) who found similar results in optical properties of mechanochemical synthesis of nanocrystalline delafossites $CuAlO_2$.Hence the assignment of the peaks for different modes of $CuAlO_2$ is a simplification of the vibrational treatment of different inorganic aluminates as well as copper complexes in organic solvents.

CHAPTER FIVE

5.0 SUMMARY, CONCLUSION AND RECOMMENDATION

5.1 SUMMARY

Thin film is a layer of material ranging from fractions of nanometer to several micrometers in thickness. It has several applications in construction such as in household mirrors and they also serve as chemical sensors that can be fabricated through the use of several types of organometallic powders dissolved in organic solvents deposited on substrate to form a heterojunction

Temperature plays a vital role in annealing for a deposited thin film. It affects the surface morphology and optical properties of the thin film.

Transparent conducting oxides are classified in to p and n-types TCOs. The p-types have unique features of optical properties in the visible light region with transparency of over 85% and optical band gap greater than 3eV and controllable electric conductivity (Kim. *et al*., 2011)

Lam, *et al*., (2009). Conducted a research on the annealing effects on the structural optical and electrical properties of $CuAlO_2$ thin film deposited on glass substrate using magnetron sputtering and found that the crystallinity of $CuAlO_2$ is improved with increasing annealing temperature in N_2 ambient.

Kim,*et al.,* (2007),conducted another research on optical and electrical properties of p-type transparent conducting oxide $CuAlO_2$ thin film deposited on Si substrate using e-beam evaporation and found the transmittance varies from 20-85% and resistivity from $5x10^{-3}$ to 4Ωcm with wet oxidation condition and an estimated optical band gap in the range of 3.96-4.20eV.

Arghya, *et al.,* (2010) conducted another research on wet chemical dip coating preparation on $CuAlO_2$ Si and glass substrate. XRD pattern confirms the crystalline phase formation with strong (006) orientation while uv-vis shows high transparency of the film in the region with direct band gap of 3.85eV.

Banerjee, *et al., (*2005) conducted a similar research on the size dependent optical properties of sputter deposited nanocrystalline p-type transparent $CuAlO_2$ thin film, the transmission electron micrographs reveal the formation of $CuAlO_2$ nanoparticle and x-ray diffraction shows diffraction peaks depicting rhombohedral crystal structure with band gap values of transmission and reflection as 3.94 and 3.84eV respectively.

In this work $CuAlO_2$ thin film wasdeposited on a glass substrate using chemical solution deposition technique out of which four samples S1, S2, S3 and S4 were produced and then annealed at temperatures 400°C, 500°C, 600°C and 700°C respectively. A study of the surface morphology was conducted on all the annealed samples, and four micrographs were produced, they all have a smooth surface with finer grains; well define grain boundaries, with dense granular structure and some voids visible in the micrographs of samples 4.3 and 4.4 It was also observed that densification of the micrographs of samples 4.1 and 4.2 has not fully taken place and that there is an improved crystallinity in samples 4.3 and 4.4, so annealing at higher temperature improves film crystallinity.

In the UV-Vis spectrophotometry the absorbance of all the four samples decreases with an increasing annealing temperature while the transmittance and absorbance absorbances of the samples increases with an increasing annealing temperature and the photons energy become sufficient to excite electrons to move from valance to conduction band.

The absorption coefficient (α) are calculated from the transmittance data using the method of (Manifacier *et al.,* 1976).The absorption coefficient decreases with increasing annealing temperature and a band gaps of 3.55eV for S1 and S2 each and 3.80eV and 3.85eVfor samples S3 and S4 respectively. And lastly the extinction coefficient is calculated from the relation k = $\frac{\lambda\alpha}{4\pi}$ and it decreases at about 4.05eV. In the Fourier transform infrared FT-IR, the analysis was carried out on sample annealed at 700°C, because the UV-Visible covers all the samples and the parameters such as transmittance, reflectance and absorbance were fully discussed

5.2 CONCLUSION

Chemical solution deposition of transparent $CuAlO_2$ thin film on clean glass microscope slide $CuAlO_2$ substrate was successfully carried out; Five samples of the $CuAlO_2$ thin films were produced out of which four samples were annealed at temperatures of 400°C, 500°C, 600°C and 700°C respectively. The surface morphology of the annealed samples was studied with the aid of a scanning electron microscope (SEM Hitachi S-1100). The micrographs also revealedthe portion of the samples studied as 720nm each. A smooth surface with finer grains and well defined grain boundaries was observed in all the four samples, some bigger clusters was also observed on the micrographs of samples S3 and S4 which resulted due to the agglomeration of finer grains and some voids are visible on the surface of micrographs of figs. 4.1 and 4.2, it was also observed that the crystallinity of samples S3 and S4 has been improved it will now be concluded that annealing at higher temperature improves crystallinity of $CuAlO_2$ thin film.

For the uv-vis and FT-IR Spectroscopy the findings indicate that while absorbance and absorption coefficient/extinction coefficients of the deposited films decreases with increasing annealing temperature, transmittance spectra exhibits that $CuAlO_2$ are transparent (37%-87%) in

the visible range, reflectance and direct band gaps of the films increases with increasing annealing temperature. And also there is an improvement in crystallinity of the deposited films as annealing temperature increases. The high direct band gap for samples S1, and S2, is about 3.55 each, while that of S3, and S4 are approximately 3.80eV and 3.85eV respectively. It can therefore be concluded that while the absorbance, absorption/extinction coefficients of $CuAlO_2$ thin film is inversely proportional to annealing temperature the transmittance, reflectance and direct band gaps are directly proportional to the annealing temperature, this therefore indicates the suitability of $CuAlO_2$ in optoelectronic technology.

5.3 RECOMMENDATIONS FOR FURTHER RESEARCH

1. Use of other substrates like conducting glass and silicon is recommended and surface morphology optical and electrical characterization should be included and comparison be made.

2. It is also recommended that the annealing temperature range for a similar research should exceed the range used in this work and the result obtained be compared with the result of this work, this will help to indicate and find out a more suitable annealing temperature for $CuAlO_2$thin film fabrication.

3.It is also recommended that XRD be conducted in a similar research to this work and the UV-Vis spectrometry should also include real and imaginary dielectric constants and the refractive index.

REFERENCE:

Arghya, B., Kalyan, K., & Chattopadhyay, K. K (2010). wet chemical dip coating preparation of highly oriented copper aluminium oxide thin film and its opto-electrical characterisation. *pp22-34 ElsevierISSN:0921-4526 Gyongsan : Yeungnam press.*

Bernerjee, A. N; Chattopadhyay k. k (2005). Recent developments in the emerging field of crystalline p-type transparent conducting oxide thin films. *Journal of progress in crystal Growth characterisation of Materials.Vol.50 pp.52-105*

Brault, J. W. (1996). New approach to high-precision Fourier transform spectrometer design. . *Applied optics.Vol.35 issue 16 pp.2891-2892 doi:10.1364/AO.35.002591*

Bryce, R (2003). Optical characterisation of sputtered $CuAl_2O$ thin film on glass substrate for solar cell application *pp 45-58 Elsevier ISSN 0934-6439 Yeungnam press*

Cachet, H., Gamard, A; Campet, B; Jousseume, B. and Toupance T. (2001). Tinoxide thin films prepared from a new alkoxyflourotin complex. *Elsevier: vol.388. pp41-49. doi:10.1016/50040-6090*

Chen, M. P. (2000). Surface characterisation of transparent conductive oxide Al-doped films. *Journal of chrystal growt,vol.33 pp. 220, 254-262*.

Christiana, H; Mato, K; Anand, K; Ulrich, G. Holgen, J. Kornelius, N. (2006). Atomic layer deposition on Biological Macromolecules: Metal oxide coating of Tobacco Mosaic Virus and Ferritin. *ACS Journals 66(6) pp.1172-1177 doi:10.1021/nl0604413j*

Coppo, P; Schroeder, R; Grell, M. and Tuner, M. L (2004). Investigation of solution processed poly Thin Films as Transparent conductors" *Synthetic Metals 143(2): 203 doi:10.1016*

Franscombe, M. H and Vossen, J. L. (1989) Hand book of thin film deposition, processes and techniques *Vol. 14 pp 25-48 Boston Academic Press.*

Ghosh, C. K; Popuri S. R; Mahesh, T. U. and Chattopadhyay, K. (1989) Preparation of Nanocrystalline $CuAlO_2$ through Sol-Gel ROUTE. *Journal of Sol-Gel science and Technology, 52(1).75-81 doi:10.1007/s10971-009-1999-x*

Griffths, P.& Hasseth, J. A. (2007). Fourier transform infrared spectrometry.*2nd ed.John Wiley and sons Inc. publication ISBN:978-0-471-19904*

Hanoar, D., & Triani, G. a. (2011). Morphology and photocatalytic activity of highly oriented mixed phase titanium dioxide thin film. *Surface and coating Technology 205(12) 3659-3664-2011*

Hartnagel, H. L., & Jain, A. K. (1995). Semiconducting transparent thin films.1st ed.ISBN:13: 978-0750303224

Horie, M., Fujiwara, N., Kokuba, M., & Kondo, N. (1994). Proceedings of instrumentation and measurement technology.*SMPTE Journal vol.102 issue 9 pp827-827 doi:10.5594/j00595*

Kawazoe, H., Yasukawa, M., Hyodo, H., Kurita, M., & Yanagi, H. a. (1997, June). P-type Electrical conduction in tranparent thin film of CuAuO2.*Nature389, 939-942.*

Kim, D. S., Park, S. J., Jeong, E. K., & Lee, H. K. (2007). optical and electrical properties of p-type transparent conducting CuAlO2 thin. *Thin solid films.vol.515 No.12 pp.5103-5108DO:10.1016/j.tsf.2006.10.044*

Kim, H. M., & Bae, K. a. (2011). Electronic and optical properties of Indium Zinc oxide thin film prepared by using Nanopowder target. *Japanese journal of applied physics .Vol.50 No.4R pp.5103-5108 IOP publshers*

Klein, T., & Buhr, E. a. (2012). A review of scanning electron microscope in transmission mode and its applications. *Cambridge Journal of Microscopy and microanalysis. Vol.20/issue01. pp.124-132*

Lambert J. H. (2006). Photometry on the measure and gradations of light, colors and shade vol.86 pp78-88

Lan, W., Cao, W. L., Zhang, M., Liu, X. Q., Wang, Y. Y., & Xie, E. Q. (2009). Annealing effect on the structural, optical and electrical properties of CUAlO2 films deposited by magnetron sputtering. *Journal of material science.Vol.44, issue 6, pp.1594-1599*

Mammah, S., Opara, F. E., Benjamin, V. O., & Ntibi, J. E. (2005). Annealing effect on the optical and solid state properties of cupric oxide thin film deposited using aqoues chemical growth. *Journal of chrystal growt,vol.41 pp. 3412-3516*

Mardare, D., Tasca, M., & and Rusu, G. I. (2000). On the structural properties and optical Transmittance of TiO2 R.F Sputtered thin films.*Journal ofApplied science, Vol.156 issue 1. pp. 200-206.*

McMullan, D. (2006). An improved scanning electron microscope for opaque specimen.*Vol.133 issue 3 pp.324-345*

Manifacier, J.C; Gasiot, J and Fillard, J. P. (1976). Envelope method analysis of a thin film with uniform thickness and complex refractive index.*Journal of physics. E.Sci.intrum. Vol.9 1002 University ofNew South Wales press.*

Minami, T. (2005). Transparent conducting oxide semiconductors for transparent electrodes.*Semiconductor science and Technology. Vol. 20 issue 4. IOP Publishing Ltd.*

Misra, P. and Dubinskii, M. A. (2002). Ultraviolet spectroscopy and UV lasers *2nd ed. issue 2. pp 257-309*

Nishikida, K; Nishio, E; and Hannah, R. W. (1995). Selected applications of FT-IR technique.*Gordo breach PP.240 CRC press.*

Prakash, I; Padma, K; Kavitha, P; and Ramasamy, S. (2008). Dielectric relaxation studies of nanocrystalline CuAlO2 using modulus formalism.*Journal of applied Physics. Vol.102 Issue 104104 doi:10.506311.2815633.*

Roy, B., Ode, A., Readey, D., Perkins, J., Parilla, P., Tepliin, C. K., (2003). Towards high performance p-type tranparent conducting oxides.*Conference paper presented at National center for photovoltaics and solar program. Review meeting. Denver Colorado.*

Sato, H., Minami, T., & Takata. S and Yamada, T. (2003). Transparent conducting p-type thin film prepared by magnetron sputtering; *Journal of thin solid film. Vol.236, pp.27-31*.

Sheng, S., & Fang, G. L. (2006, April). P-type transparent conducting oxide. *Journal ofmateriak chemistry Issue23203, doi:10.1039/C5Tc0170E*

Sheshan, K. (2012). Handbook of thin film deposition*3rd ed. (Vol. III). PP.408 ISBN: 978143777873Amsterdam.*

Skoog, D. A., Holler, F., & James, C. a. (2007). Principles of instrumental analysis*(6th ed.). ISBN: 10:0495012017Thomson Brooks /cole.*

Smith, B. C. (1999). Infrared spectral interpretation Vol.II Issue 4CRC press.

Sunyoung, S., Yoon, S. H., & and Hwa-Min, K. (2011). Transparent conductive oxide (TCO) films for organic light emissive devices.*Journal of material processand devices.ISBN:978-953-307-279 doi: 10.5771/18545*

Tanooka, k. S. and Kikuchi, N. (2002). Thin films grown by flux mediated solid phase. *Journal of Thin solid films. vol.411 pp.1-232*

Thomas, G. (1997). Invicible circuit *Transparent electronics. Nature 389:907-908*

Wang, Y. (2003). P-type transparent conducting Cu-Al-O thin films prapared by PE-MOCVD.*Nature 389.*

Weast, R. C . (1975). Hand book of chemistry and physics *56th edition pp 489-491 ISBN:10:039501301*